

Generation of a broadband xuv continuum in high-order-harmonic generation by spatially inhomogeneous fields

I. Yavuz,^{1,*} E. A. Bleda,¹ Z. Altun,¹ and T. Topcu²¹*Department of Physics, Marmara University, 34722 Ziverbey, Istanbul, Turkey*²*Department of Physics, Auburn University, AL 36849-5311, USA*

(Received 6 December 2011; published 27 January 2012; corrected 3 February 2012)

We address an efficient scheme to generate a broadband extreme-ultraviolet (xuv) continuum from high-order harmonic generation emerging from the concept of plasmonic field enhancement in the vicinity of metallic nanostructures [Kim *et al.*, *Nature (London)* **453**, 757 (2008)]. Based on the numerical solution of a time-dependent Schrödinger equation, for moderate field intensities and depending on the inhomogeneity of the field, we are able to increase the plateau region roughly by a factor of two and generate a broadband xuv continuum. The underlying physics of the plasmon enhancement in harmonic generation is investigated in terms of the semiclassical trajectories of strong field-electron dynamics, and perfect consistency is found between quantum mechanical simulations. It is found that the field inhomogeneity plays a critical role in quantum path selection. After a critical value, we observe a systematic suppression in the long trajectories, suggesting the generation of a single isolated attosecond pulse. Finally, we investigate the dependence of cutoff position on the order of field inhomogeneity and find a $\beta^{2.3\mp 0.2}$ scaling.

DOI: 10.1103/PhysRevA.85.013416

PACS number(s): 32.80.Rm, 42.65.Ky, 78.67.Bf

I. INTRODUCTION

High harmonic generation (HHG) is one of the most attractive methods to understand the interaction of intense laser fields with matter. It is of the paramount importance and is still a rapidly growing field due to its potential to produce coherent radiation sources covering a range from vacuum ultraviolet (VUV) to the soft x-ray region and to generate attosecond pulses [1]. The HHG process can be described in terms of the so-called three-step (or *simple man's*) model [2]; in this process, the electron first tunnels through the atomic potential barrier suppressed by a driving laser field and accelerates, and then the subsequent motion of the electron in the continuum is treated classically. When the electric field reverses its sign, the electron gains kinetic energy and recombines with its parent ion and radiates energetic photons. The highest kinetic energy that the electron gains at the continuum is determined by $E_{\max} = 3.17U_p$, where $U_p = E_0^2/4\omega_0^2$ is the ponderomotive potential. The highest harmonic frequency that can be gained from this process is defined by the cutoff formula [2]

$$q_{\max}\omega_0 \simeq I_p + 3.17U_p, \quad (1)$$

where I_p is the ionization potential. One of the major branches of HHG studies has focused on the optimization of HHG efficiency or extending the plateau region needed in many applications such as mapping of attosecond electron wave-packet motion [3] or tomographic orbital imaging [4]. This is mostly achieved by modifying driving a laser pulse shape such as by multicolor driving [5,6] or controlling macroscopic parameters such as pressure, focus position, and medium size [7]. However, in recent years an alternative technique has emerged, field enhancement in the vicinity of metallic nanostructures, has attracted much attention by investigators over the years both experimentally [8] and theoretically [9]. Field enhancement from metallic nanostructures is achieved by localization of

a femtosecond radiation in a nanometer-scale confinement with no extra cavity. In addition, the field enhancement largely depends on the geometrical shape of the metallic nanostructure [8]. In a recent experiment by Kim *et al.* [8], in the vicinity of the bow-tie-shaped nanostructure, the driving laser field is enhanced up to three orders of magnitude between the vertices. Thus, for field intensities well below the HHG threshold, it has been possible to generate the 17th (47 nm) harmonic of an argon gas jet. The underlying mechanism of the plasmon field-enhanced HHG can be described as follows: A bow-tie-shaped nanostructure, which has a gap of 20 nm, is irradiated by a femtosecond laser pulse with a low intensity, and negative charges are redistributed around one apex and positive charges around the other one; thus a hot spot of a highly enhanced field is generated. Consequently, when a gas jet is injected to this hot spot, an enhanced HHG spectrum is efficiently generated. One of the first systematic theoretical investigations of the plasmonic field enhancement in the vicinity of metal nanostructures was provided by Husakou *et al.* [9] using a modified version of the Lewenstein model in such a way that the field inhomogeneity and electron absorptions from metal surfaces are incorporated. They demonstrated that up to three-orders-of-magnitude enhancement in the field intensity can be achieved, in accordance with Ref. [8]. Furthermore, due to the broken symmetry of the interacting potential, for a moderate field intensity, they observed even harmonics along with odd harmonics up to fifth order. Ciappina *et al.* [10] have characterized plasmonic field enhancement in HHG using the modified version of the Lewenstein model, a one-dimensional time-dependent Schrödinger equation, and semiclassical trajectories and described the reasons for the cutoff extension.

In this study we perform a numerical analysis to generate a spectrum with broadband continuum harmonics from an inhomogeneous field in analogy with the field enhancement in the vicinity of a bow-tie-shaped nanostructure, taking the target atom as a hydrogen atom. The key idea here is to consider the driving laser field so that it has a spatiotemporal

*ilhan.yavuz@marmara.edu.tr

distribution. The conventional techniques to generate high-order harmonics are generally through the interaction of, what is assumed to be, homogeneous laser fields and gas jets. However, due to strong confinement of the generated hot spots, we should treat the interacting field as inhomogeneous. On the other hand, if the driving laser field is as short as a few femtoseconds, it is possible to obtain a single burst of radiation, and a continuum of high-order harmonics can be generated. Thus, from the superposition of a number of extreme-ultraviolet (xuv) continuum harmonics a single isolated pulse of attosecond duration can be generated. If we consider the driving field as inhomogeneous and the target atom at the gap of the nanostructure, the constructive electron trajectories that generate the harmonics around the cutoff position would gain much high kinetic energy before returning back to its parent ion. Therefore, the plateau region should be extended, since the harmonic frequencies are proportional to the kinetic energy of returning electron.

Many schemes have been proposed theoretically to achieve single attosecond pulses from HHG. To name a few: Zeng *et al.* [11] proposed using two-color fields to generate an xuv supercontinuum in a two-color field and obtained a 65 as pulse; Merdji *et al.* [12] demonstrated that by mixing the fundamental field with its detuned second harmonic an 80 as pulse can be obtained; Zhang *et al.* [13] used a two-color time-gating laser field and attained a 96 as pulse; Zhang *et al.* [6] showed that by adding an xuv pulse to a synthesized two-color field a 40 as pulse can be generated; and Chen *et al.* [14] demonstrated that a 38 as pulse can be generated from two-color fields by preparing target ions in a coherent superposition of bound states.

The paper is organized as follows. Section II introduces our model of an atom interacting with an inhomogeneous femtosecond laser pulse. The method to solve is the time-dependent Schrödinger equation, and useful physical observables are described in this section. In Sec. III the influence of inhomogeneity on the spectral as well spectrotemporal profile of HHG, carrier-envelope-phase effects on cutoff position, and temporal variation of attosecond pulses for different inhomogeneities are discussed. Unless otherwise stated, atomic units are used throughout this paper.

II. THEORETICAL METHOD

The interaction of hydrogen with an intense laser field can be modelled by solving the time-dependent Schrödinger equation (TDSE) in the length gauge,

$$i \frac{\partial \psi(\vec{r}, t)}{\partial t} = \left[-\frac{1}{2} \nabla^2 - \frac{1}{r} + W(\vec{r}, t) \right] \psi(\vec{r}, t), \quad (2)$$

where $W(\vec{r}, t)$ represents the interaction term. We assume that the field is linearly polarized along the z axis. Due to the spatial dependence of the laser field, we model the interaction term $W(\vec{r}, t)$ by [9]

$$W(\vec{r}, t) = \vec{r} \cdot \vec{E}(t) = E_0 z (1 + \beta z) f(t) \cos(\omega_0 t + \phi_{\text{CEP}}), \quad (3)$$

where E_0 is the amplitude, ω_0 is the frequency, and ϕ_{CEP} is the carrier-envelope phase (CEP) of the driving field. The driving wavelength is taken to be 800 nm. Unless otherwise stated, ϕ_{CEP} of the field is set to zero. The parameter β determines

the order of inhomogeneity of the field and its unit is in the reciprocal length. We use a sin-squared envelope $f(t)$, and the duration of interaction is four cycles (roughly 11 fs). To solve Eq. (2) numerically, we assume that the total electronic wave function can be expanded in terms of spherical harmonics times radial functions [15]:

$$\psi(\vec{r}, t) = \sum_{l=0}^L \frac{R_l(r, t)}{r} Y_l^0(\theta). \quad (4)$$

We assume that the driving field is linearly polarized along the z axis, and the target atom is in the $1s$ (ground) state. Thus, we take $m = 0$. If we insert Eqs. (3) and (4) into Eq. (2) and recall that

$$\cos \theta Y_l^0 = c_l Y_{l+1}^0 + c_{l-1} Y_{l-1}^0 \quad (5)$$

and

$$\cos^2 \theta Y_l^0 = c_l c_{l+1} Y_{l+2}^0 + (c_l^2 + c_{l-1}^2) Y_l^0 + c_{l-1} c_{l-2} Y_{l-2}^0, \quad (6)$$

we obtain a set of coupled differential equations for the radial functions of the form

$$\begin{aligned} i \frac{dR_l(r, t)}{dt} = & \left[-\frac{1}{2} \frac{\partial^2}{\partial r^2} + \frac{l(l+1)}{2r^2} - \frac{1}{r} \right] R_l(r, t) \\ & + r E(t) \{ c_l R_{l+1}(r, t) + c_{l-1} R_{l-1}(r, t) \\ & + \beta r [c_l c_{l+1} R_{l+2}(r, t) + (c_l^2 + c_{l-1}^2) R_l(r, t) \\ & + c_{l-1} c_{l-2} R_{l-2}(r, t)] \}, \end{aligned} \quad (7)$$

where c_l is the coupling coefficient and has the form

$$c_l = \sqrt{\frac{(l+1)^2}{(2l+1)(2l+3)}}, \quad (8)$$

and $E(t) = E_0 f(t) \cos(\omega_0 t + \phi_{\text{CEP}})$. We see from Eq. (7) that each angular momentum channel l is coupled by the laser field to $l \mp 1$ states as well as $l \mp 2$ states. Therefore, unlike conventional numerical solution techniques of TDSE, in our case, at each time step we need to deal with pentadiagonal matrices in l coordinates. Equation (7) can effectively be solved by using well-known split-operator method [15]. In our calculations we found that a radial grid with a maximum radius of 300 a.u., grid spacing of 0.1 a.u., and maximum number of partial waves of $L_{\text{max}} = 100$ –200 is sufficient to obtain converged results. The time step is $1/16384$ of an optical cycle. In order to prevent spurious reflections from a radial grid boundary, at each time step, the total wave function is multiplied by a mask function of the form $\cos^{1/8}$, which varies from 1 to 0 starting from the $2/3$ of the grid. Moreover, the mask function guarantees the absorption of the components of the wave packet from the surface of the nanostructure, which does not contribute to HHG. The photoemission spectrum is calculated from the Fourier transform of the dipole acceleration $a(t)$.

III. RESULTS AND DISCUSSION

In this section we will investigate the effect of inhomogeneity on the spectral profile of the high-order harmonic spectrum. The typical intensity of the inhomogeneous field is taken to be 300 TW/cm², and the duration of the laser field is four cycles.

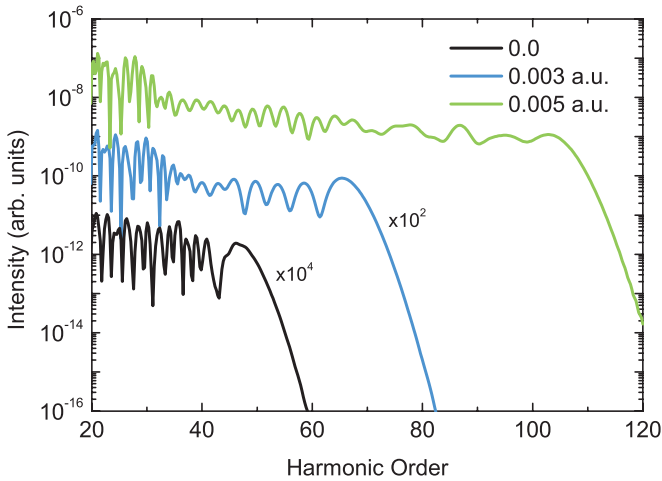


FIG. 1. (Color online) The effect of β inhomogeneity parameter on the harmonic spectrum from hydrogen atom initially in the ground state. The laser field is sin-squared, four cycles, with a peak intensity of 300 TW/cm^2 and wavelength of 800 nm . As the β parameter increases the plateau region is extended. The HHG spectra obtained for $\beta = 0.0$ and $\beta = 0.003 \text{ a.u.}$ are scaled for clarity.

The CEP ϕ of the driving field is taken as 0. We choose a set of different values of the β parameter between 0 and 0.005 a.u. . The black line in Fig. 1 shows the harmonic spectrum obtained from a hydrogen atom when $\beta = 0 \text{ a.u.}$, which corresponds to a homogenous field. As can be seen from this curve, the cutoff position is at the 46th harmonic, which corresponds to a photon of 71 eV energy. The frequency of the highest harmonic fits the cutoff law, given in Eq. (1), assuming that the spatial distribution of the driving field is homogenous. As shown in Fig. 1 by the blue (gray) curve, as we set the β parameter to 0.003 a.u. (which corresponds to an inhomogeneity region of 17.6 nm), we observe a substantial increase of the plateau region in agreement with the experiments of Kim *et al.* [8]. On the other hand, since the pulse duration is short and due to the temporal profile of the driving field, the peaks that appear near the cutoff are not harmonic, whereas their separation increases with the harmonic order. This is the result of the interference between short and long quantum paths, which creates relatively large modulation, shown in Fig. 1 by the blue (gray) line. The nonharmonic behavior lies in the fact that during the HHG process the cutoff harmonics are emitted only once, and a single burst of radiation is produced. Moreover, due to field inhomogeneity the electrons that are released around the maximum of the driving field are further reaccelerated in the continuum and gain extra kinetic energy—compared with the homogenous field—before recolliding with their parent ions. As can be seen from the same figure, as we increase the β parameter to 0.005 a.u. the plateau region is further extended, as would be expected. In this case the position of the cutoff is at the 103th harmonic. However, one can see from the green (light gray) curve in Fig. 1 that the spectral profile of the harmonics between 60 and 103 are much smoother than the spectrum obtained from $\beta = 0.003 \text{ a.u.}$ This is evidence of a strong quantum path selection and is the key idea in generating isolated attosecond pulses. It is known that a broadband xuv continuum can be generated if one of the

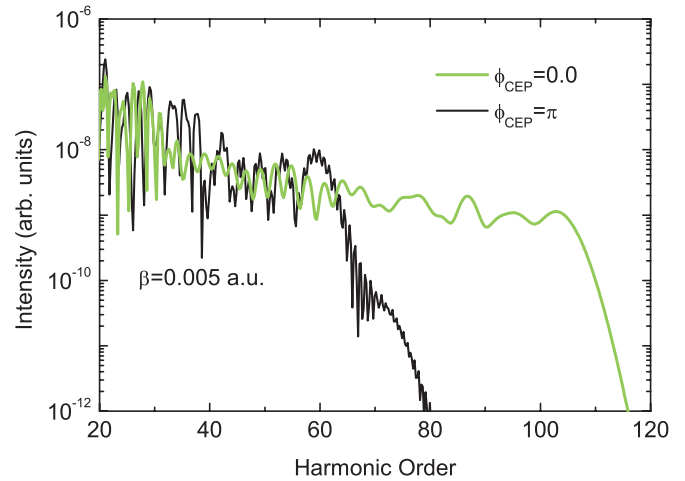


FIG. 2. (Color online) Dependence of the field inhomogeneity on the carrier-envelope-phase (CEP) of the driving field. We choose two different CEP values, 0 and π . β is set to 0.005 a.u. The field parameters are the same as in Fig. 1.

electron paths (between a long and short path) that contributes to the harmonic spectrum is favored. Due to the wave-packet diffusion effects a reasonable selection would be to favor the short quantum path.

For short laser fields, whose durations are on the order of a few femtoseconds, the CEP of the field is primarily important [16]. In view of this, we investigate the dependence of HHG driven by an inhomogeneous field on CEP. We use two different CEP values, $\phi_{\text{CEP}} = 0$ and $\phi_{\text{CEP}} = \pi$. First, the harmonic spectra observed for $\phi_{\text{CEP}} = 0$ and $\phi_{\text{CEP}} = \pi$ would be exactly the same for homogeneous fields due to the inversion symmetry. However, for fields where $\beta \neq 0$, the inversion symmetry is predominantly broken [9]. In this aspect, we set $\beta = 0.005 \text{ a.u.}$ and solved Eq. (2) with these two CEP values. The results are presented in Fig. 2. The green (light gray) line seen in this figure is the same spectrum presented in Fig. 1, which corresponds to $\phi_{\text{CEP}} = 0$. However, when ϕ_{CEP} is set to π , the HHG spectrum dramatically changes. The cutoff position shrinks back to 70th harmonic, and its efficiency considerably reduces. A large modulation occurs between 40th and 60th harmonics. The dramatic difference in the spectral profile due to CEP arises from the fact that, while the laser field sweeps the atom, the sign of the charge distribution seen by an active electron differs from $\phi_{\text{CEP}} = 0$ to $\phi_{\text{CEP}} = \pi$. In other words, during the time of the emission of the cutoff harmonics, when $\phi_{\text{CEP}} = 0$ the released electron experiences a Lorentz force from the field with a positive sign and is reaccelerated before recombining with its parent ion. On the other hand, when $\phi_{\text{CEP}} = \pi$ the electron experiences the field with a negative sign, which screens the electron motion in the continuum. This results in the reduction of the cutoff harmonics.

In order to obtain a deeper insight into the effect of inhomogeneity on the HHG process, the harmonic spectra are analyzed in terms of time-frequency analysis [17]. Figure 3 presents the time-frequency distribution of the harmonic spectra generated from a hydrogen atom. The upper panel represents the time-frequency distribution obtained from the

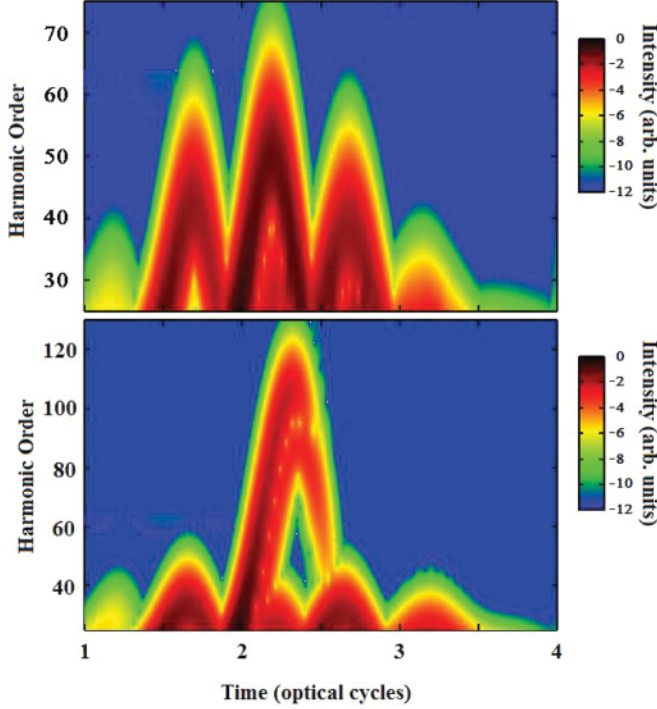


FIG. 3. (Color online) Time-frequency distribution of the HHG spectrum of hydrogen with two different β parameters. Upper panel: $\beta = 0$ a.u., lower panel $\beta = 0.005$ a.u. As can be seen from the graphs, in both cases the cutoff harmonics are emitted only once. When β is set to 0.005 a.u., there is a substantial increase in the second peak of the three distinct peaks, and the long path contribution (right arm of the second peak) almost disappears.

homogeneous field, i.e., $\beta = 0$ a.u., and the lower panel represents the distribution obtained from $\beta = 0.005$ a.u. As can be seen from the upper panel, there is an evidence of a quantum path interference, which brings out the irregular spectral structure shown in Fig. 1 with the black curve. Although there seem to be three noticeable peaks (between 1.5 and 2.0, 2.0 and 2.5, and 2.5 and 3.0 optical cycles) in the distribution, the leading contribution to the harmonic spectrum is between the 2 and 2.5 optical cycles, whereas the strength of the long and short quantum paths (right and left arms of the peak, respectively) is almost at the same order. However, when the inhomogeneity of the driving field is increased to $\beta = 0.005$ a.u. the time-frequency distribution of harmonic spectrum reveals distinct features compared with the homogeneous field. First, the profiles of the first and the third peaks are almost maintained, suggesting a negligible effect of the inhomogeneity of the field. On the other hand, there is a dramatic increase in the remaining peak due to the effect of the field inhomogeneity as well as the broken inversion symmetry. In this case during the time when the electron propagates in the continuum, it acquires larger kinetic energy before reaching the parent ion and very energetic photons should be emitted. An analogous effect of broken inversion symmetry in the HHG process has been pronounced for a combined linearly polarized laser field and a static field, where it is possible to observe even and odd harmonics as well as an extended, multiple plateau structure [18,19]. With a closer look we can see from the highest peak in the lower panel of Fig. 3 that the intensity of

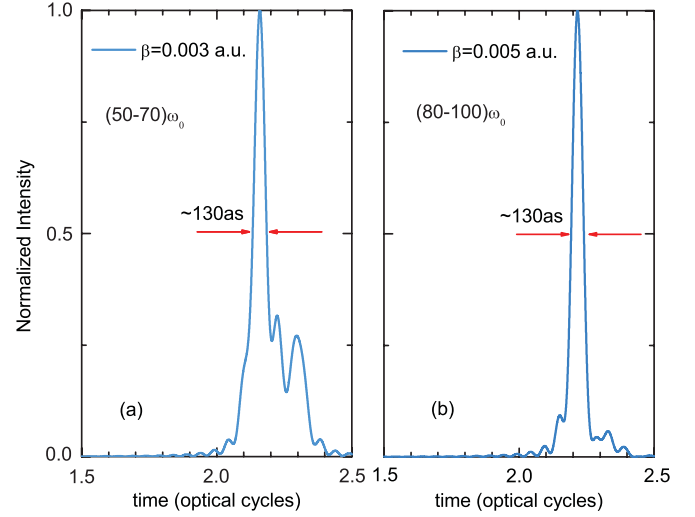


FIG. 4. (Color online) Temporal variation of the attosecond pulses generated from hydrogen atoms. (a) β is set to 0.003 a.u., and the harmonics are chosen from the 50th to 70th orders; (b) β is set to 0.005 a.u., and the harmonics are chosen from the 80th to 100th orders. In both cases roughly a 130 as the pulse is generated. However, for $\beta = 0.005$ a.u. the irregular satellite pulses are largely suppressed.

the long path (right arm of the highest peak) is almost removed compared with that of the short path (left arm of the highest peak), suggesting a generation of an isolated attosecond pulse in that region.

Next, we investigate the attosecond pulse generation in the inhomogeneous field by superposing a number of harmonics near the cutoff of the HHG spectrum. As shown in Figs. 4(a) and 4(b), for $\beta = 0.003$ and 0.005 a.u. we select the harmonics between the 50th and 70th and the 80th and 100th orders, respectively. In both cases the bandwidth of the continuum is 20 harmonics, and the intensities of the pulses in both figures are normalized to unity. The durations of the generated attosecond pulses given in Figs. 4(a) and 4(b) are roughly 130 as. However, the differences in these graphs are the satellite pulses around the main pulses, which arise from the long path. For $\beta = 0.003$ a.u. there is a distinct contribution from the long path, which causes an irregular structure seen around the main pulse. However, these irregular structures are largely suppressed when β is set to 0.005 a.u., and a clean isolated 130 as pulse is generated.

The underlying physical mechanism of HHG can be understood in terms of a semiclassical three-step model [2]. In this model the motion of the electron under the action of the linearly polarized inhomogeneous laser field is described by

$$\ddot{z}(t) = -dW(z,t)/dz. \quad (9)$$

It is assumed that electron is lifted to the continuum at $z = 0$ with zero velocity, i.e., $\dot{z}(t) = 0$, at the release time t_i and recombines at the recombination time t_r . We vary the release time t_i and solve Eq. (9) to investigate the laser-driven electron trajectories in a inhomogeneous field using a velocity Verlet algorithm [20]. Thus, the kinetic energy of the returning electron can be found from $E_k(t_r) = \dot{z}^2(t_r)/2$. The form of $W(z,t)$ in this equation is given in Eq. (3). In semiclassical

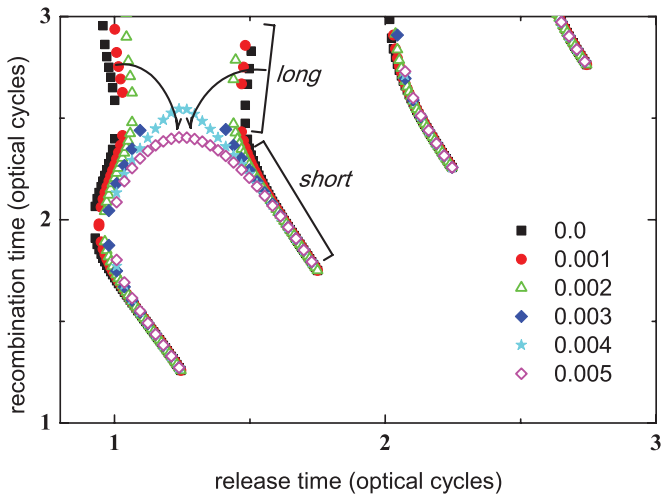


FIG. 5. (Color online) Dependence of the recombination time on the release time of the semiclassical trajectories for different values of β parameter. The field parameters are the same as in Fig. 1. Note the substantial variation of the long path released between 1.0 and 1.5 optical cycles.

simulations, we assure that the electron trajectories that result from absorptions from the metal surfaces do not contribute to harmonic emission. In Fig. 5 recombination time of the electron is presented as a function of the release time of the electron for several values of β between 0.0 and 0.005 a.u. We first focus on the release time interval between the first and second optical cycles. We have marked the times of short and long paths on this figure. Figure 5 shows that the release and recombination times of the short trajectories are almost independent of β , but there is systematic mutation in the long path contribution. The recombination times of the long path released around the first cycle and around the 1.5th cycle embrace as the inhomogeneity of the laser field increases, as shown by the bent arrows. This indicates that the recombination times of the short and long trajectories would be in phase. However, the long trajectories released around the 1.5th optical cycle predate to the first optical cycle; hence, their flight times in the continuum increase. This results a substantial decrease in the intensities of the long trajectories due to quantum diffusion effects [21] and may explain the vanishing long trajectories seen in the lower panel of Fig. 3. In fact, the reason for the decrease in the intensities is threefold. First is the wave-packet diffusion effect, as we have already mentioned. The other (and major) reason lies from the fact that, by virtue of the three-step model, the field strength at the time of ionization is lower for long trajectories (first optical cycle) than for short trajectories (1.5 optical cycles). Since the tunneling ionization rate is a highly nonlinear function of the laser electric field amplitude at the ionization time, the efficiency of the long trajectories would be much lower than that of the short trajectories. Another reason is the probability of a nonzero initial velocity of the ionized electron [19], which cannot be analyzed in terms of a semiclassical three-step model, since the ionized electron is constrained to have zero velocity initially.

In Figs. 6(a) and 6(b), the dependence of harmonic orders on the release time and recombination time of the electron

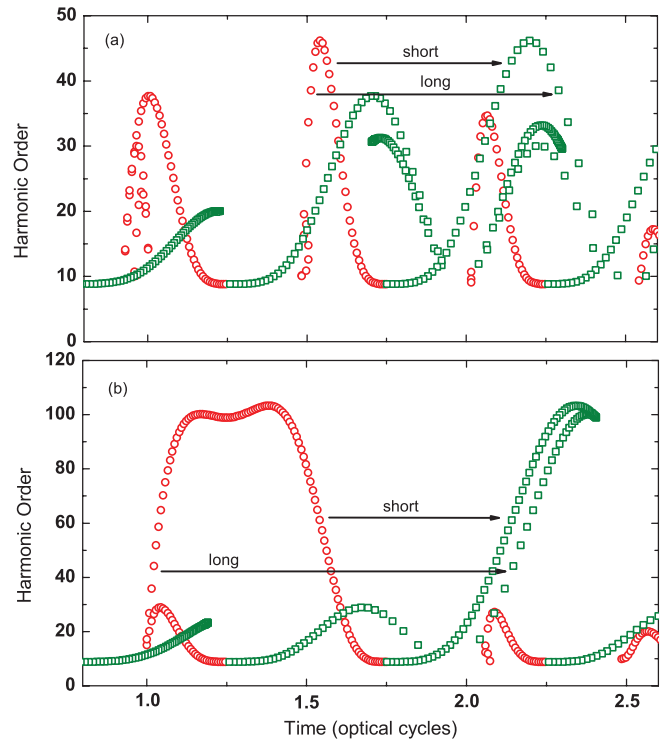


FIG. 6. (Color online) Dependence of harmonic order on the release time (\circ) and the recombination time (\square) of the electron. (a) $\beta = 0$ a.u.; (b) $\beta = 0.005$ a.u. The parameters are the same as in Fig. 1.

is investigated for two different inhomogeneity parameters, $\beta = 0.0$ a.u. and $\beta = 0.005$ a.u. In Fig. 6(a) $\beta = 0.0$ a.u. corresponds to a homogeneous field. For this case, the electron releases near every half cycle and contributes to the formation of harmonic spectrum. The left and right arms of these peaks have positive (short path) and negative (long path) slopes with different emission times. Maximum harmonic frequency of $46\omega_0$ is consistent with the cutoff position shown in Fig. 1 with the black curve. For $\beta = 0.005$ a.u., first, one can see roughly a factor of 2 increase in the maximum harmonic frequency, which is $103\omega_0$. This is again consistent with the cutoff position given in Fig. 1 with a green (light gray) curve. On the other hand, except for their contributions to the harmonic spectrum, the short trajectories that are released around 1.5 cycles and recombined between 2.0 and 2.5 cycles are almost identical in Figs. 6(a) and 6(b). This may be the reason why the efficiencies of the harmonic spectra presented in Fig. 1 are almost maintained for different β values. As can be seen from Fig. 6(b), long trajectories of the main peak are released near the first cycle, which is roughly a half cycle earlier than that of $\beta = 0$ a.u. and recombines between the 2 and 2.5 optical cycles with a positive slope. However, as described above, since the flight times of the long trajectories are larger than the short ones, the efficiency of the long trajectories are much lower. This suggests that the short path can be selected efficiently at a proper β of inhomogeneity to generate a broadband xuv continuum and a single isolated attosecond pulse.

Finally, we investigate the dependence of the cutoff on the field inhomogeneity β of the driving field. The β values are chosen between 0.0 and 0.005 a.u. on a coarse mesh with

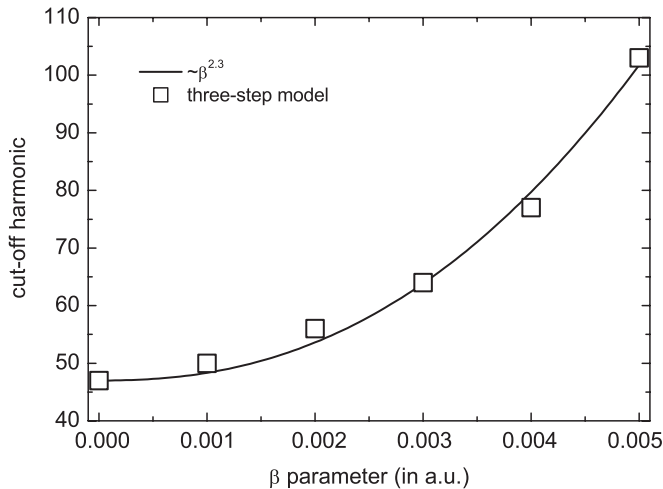


FIG. 7. The variation of the cutoff position of HHG as a function of field inhomogeneity β between 0.0 and 0.005 a.u. The nonlinear fit has the form of β^x . The parameters are the same as in Fig. 1.

0.001 a.u. The results are presented in Fig. 7. As shown in this figure, the increase in the order of the inhomogeneity does not translate into the cutoff extension linearly; rather there is a nonlinear variation in the cutoff position as a function of the field inhomogeneity in agreement with Ref. [9]. A simple nonlinear fit to an analytic function shows that the increase of the cutoff position scales as $\beta^{2.3 \pm 0.2}$. We also checked the consistency of the dependence of the cutoff position on β using classical trajectories and the solutions of the TDSE, and

results are in perfect agreement. Although it is not presented here in detail, we may say that this scaling law is not a unique expression of the effect of the field inhomogeneity on a harmonic spectrum; rather our choice of parameters (field intensity, wavelength, CEP, target atom, etc.) gives rise to obtaining this formula.

IV. CONCLUSIONS

We have theoretically proposed an alternative scheme to generate a broadband continuum in HHG by means of plasmonic field enhancement in metallic nanostructures, based on the numerical solution of a time-dependent Schrödinger equation. We used a four-cycle, 800 nm laser field with a carrier-envelope phase of zero and observed a systematic increase in the cutoff position as well as a broadband continuum with much less modulation. Our calculations showed that it is possible to select a short quantum path via suppressing a long path and to attain a 130 as pulse with a proper choice of field inhomogeneity. Our method can be considered as a possible and efficient source to generate a coherent radiation with an attosecond duration.

ACKNOWLEDGMENTS

I.Y. would like to thank BAPKO of Marmara University for financial support and TR-GRID of Ulakbim for computational support. T.T. was supported by the Office of Basic Energy Sciences, US Department of Energy.

-
- [1] M. Hentschel, R. Kienberger, C. Spielmann, G. A. Reider, N. Milosevic, T. Brabec, P. B. Corkum, U. Heinzmann, M. Drescher, and F. Krausz, *Nature (London)* **414**, 509 (2001).
 - [2] P. B. Corkum, *Phys. Rev. Lett.* **71**, 1994 (1993).
 - [3] H. Niikura, D. M. Villeneuve, and P. B. Corkum, *Phys. Rev. Lett.* **94**, 083003 (2005).
 - [4] J. Itatani, J. Levesque, D. Zeidler, H. Niikura, H. Pepin, J. C. Kieffer, P. B. Corkum, and D. M. Villeneuve, *Nature (London)* **432**, 867 (2004).
 - [5] K. L. Ishikawa, *Phys. Rev. A* **70**, 013412 (2004).
 - [6] G. T. Zhang, J. Wu, C. L. Xia, and X. S. Liu, *Phys. Rev. A* **80**, 055404 (2009).
 - [7] L. Roos, M. B. Gaarde, and A. L'Huillier, *J. Phys. B* **34**, 5041 (2001).
 - [8] S. Kim, J. Jin, Y.-J. Kim, I.-Y. Park, Y. Kim, and S.-W. Kim, *Nature (London)* **453**, 757 (2008), and references therein.
 - [9] A. Husakou, S.-J. Im, and J. Herrmann, *Phys. Rev. A* **83**, 043839 (2011).
 - [10] M. F. Ciappina, J. Biegert, R. Quidant, and M. Lewenstein, e-print [arXiv:1110.0665v1](https://arxiv.org/abs/1110.0665v1) [physics.atom-ph].
 - [11] Z. Zeng, Y. Cheng, X. Song, R. Li, and Z. Xu, *Phys. Rev. Lett.* **98**, 203901 (2007).
 - [12] H. Merdji *et al.*, *Opt. Lett.* **32**, 313 (2007).
 - [13] L. Zhang, Z. Zeng, X. Song, H. Xiong, Y. Zheng, R. Li, and Z. Xu, *J. Phys. B* **41**, 115601 (2008).
 - [14] J.-G. Chen, Y.-J. Yang, S.-L. Zeng, and H.-Q. Liang, *Phys. Rev. A* **83**, 023401 (2011).
 - [15] M. R. Hermann and J. A. Fleck Jr., *Phys. Rev. A* **38**, 6000 (1988).
 - [16] A. de Bohan, P. Antoine, D. B. Milošević, and B. Piraux, *Phys. Rev. Lett.* **81**, 1837 (1998).
 - [17] P. Antoine, B. Piraux, and A. Maquet, *Phys. Rev. A* **51**, R1750 (1995).
 - [18] B. Wang, X. Li, and P. Fu, *J. Phys. B* **31**, 1961 (1998).
 - [19] S. Odžak and D. B. Milošević, *Phys. Rev. A* **72**, 033407 (2005).
 - [20] W. C. Swope, H. C. Andersen, P. H. Berens, and K. R. Wilson, *J. Chem. Phys.* **76**, 637 (1982).
 - [21] M. Lewenstein, P. Balcou, M. Y. Ivanov, A. L'Huillier, and P. B. Corkum, *Phys. Rev. A* **49**, 2117 (1994).